Tracing deep-sea calcite dissolution: Agreement between the *Globorotalia menardii* fragmentation index and elemental ratios (Mg/Ca and Mg/Sr) in planktonic foraminifers

Figen Mekik[1] and Roger François[2]

[1] Accurately quantifying deep-sea calcite dissolution is crucial for understanding the role of the marine carbonate system in regulating atmospheric pCO$_2$ over millennia. We compare a foraminifer-fragmentation-based calcite dissolution proxy (*Globorotalia menardii* fragmentation index (MFI)) to Mg/Ca, Sr/Ca, and Mg/Sr in several species of deep dwelling planktonic foraminifers. We conducted microfossil and geochemical analyses on the same core top samples taken at different depths on the Ontong Java Plateau to maximize the dissolution signal and minimize the temperature overprint on our data. We also compare elemental ratios from planktonic foraminifer tests to modern bottom water $CO_3^=$ undersaturation and model-derived estimates of percent calcite dissolved in deep-sea sediments. We find clear linear decreases in Mg/Ca or Mg/Sr in *G. menardii* and *Pulleniatina obliquiloculata* with increasing (1) bottom water $CO_3^=$ undersaturation, (2) percent calcite dissolved in sediments calculated with biogeochemical modeling, (3) MFI, and (4) percent calcite dissolved derived from MFI. These findings lend further support to MFI as a calcite dissolution proxy for deep-sea sediments. In contrast, we find no significant correlation between Sr/Ca and independent dissolution indicators. Our results suggest that Mg/Ca and Mg/Sr from deep dwelling foraminifers could potentially be used as calcite dissolution proxies in combination with independent water temperature estimates. Likewise, establishing the relationship between MFI and dissolution-induced changes in the Mg/Ca of surface-dwelling foraminifers could provide a tool to correct Mg/Ca–derived sea surface temperature reconstructions for calcite dissolution.

1. Introduction

[2] The marine carbonate system acts to buffer changes in atmospheric pCO$_2$ over thousands of years. It is a complex system with many components including (1) the input of ions into the ocean through weathering on land; (2) air-sea exchange of CO$_2$; (3) the marine biological pump; (4) the ratio of organic carbon to calcite flux (rain ratio) at the seabed; and (5) the dissolution of carbonates in deep-sea sediments. Accurate estimation of the latter is thus one of the keys to understanding the evolution of the carbon cycle over geological time.

[3] Cycles in calcite content in deep-sea sediments have been observed as far back as the Challenger Expedition (J. Murray and A. Renard in 1891 cited by *Berger* [1975]). These variations can represent changes in multiple factors, such as calcite flux, fluxes of other sedimentary components and, especially, calcite dissolution. However, a reliable quantitative calcite dissolution proxy is still elusive. *Arrhenius* [1952] was the first to use foraminifer fragmen-

tation as a dissolution indicator. Many calcite dissolution indices have been proposed since then, such as the relative abundance in sediments of foraminifer species with different susceptibilities to dissolution [*Berger*, 1968, 1970; *Thompson and Saito*, 1974], the ratio of benthic to planktonic foraminifers in sediments [*Thunnell*, 1976], and the number of whole foraminifer shells per dry sediment weight [*Le and Shackleton*, 1992]. Comparing several of these proxies in the same cores, *Le and Shackleton* [1992] concluded that foraminifer fragmentation is a more robust indicator of dissolution than proxies based on foraminifer species assemblages. *Oba* [1969] found a good statistical relationship between the ratio of fragmented to whole *Globorotalia menardii* shells and benthic/planktic ratios in deep-sea sediments suggesting that *G. menardii* fragmentation may be a good indicator of calcite dissolution. Subsequent laboratory experiments [*Ku and Oba*, 1978] confirmed that dissolution damage in this species is progressive. *G. menardii* fragmentation was one of the six proxies used by *Peterson and Prell* [1985a, 1985b] to quantify calcite dissolution (see *Mekik et al.* [2002] for a detailed summary of the history of calcite dissolution proxies). Most of these early proxies were calibrated against water depth or the calcite content of dry bulk sediment.

[4] Recently, three dissolution proxies based on the morphology and fragmentation trend of planktonic foraminifer shells have been proposed: (1) carbonate size index

[1]Department of Geology, Grand Valley State University, Allendale, Michigan, USA.
[2]Department of Earth and Ocean Sciences, University of British Columbia, Vancouver, British Columbia, Canada.

[*Broecker and Clark*, 1999], (2) size normalized shell weight [*Lohmann*, 1995; *Broecker and Clark*, 2001] and (3) the *G. menardii* fragmentation index (MFI) [*Mekik et al.*, 2002]. The first two of these were calibrated against independent estimates of bottom water $[CO_3^=]$. *Emerson and Bender* [1981] and *Archer and Maier-Reimer* [1994] established that in addition to $CO_3^=$ undersaturation of bottom waters, seabed organic carbon flux significantly affects deep-sea calcite dissolution. Accordingly, MFI was calibrated with independent, model-derived estimates of percent calcite dissolved where changes in both bottom water $[CO_3^=]$ and seabed organic carbon flux were taken into account.

[5] Although MFI has provided geographically coherent calcite rain rate reconstructions in subsequent studies [*Loubere et al.*, 2004; *Mekik et al.*, 2006; also Is carbonate compensation from the last deglaciation responsible for the late Holocene increase in atmospheric pCO_2?, submitted to *Paleoceanography*, 2006, hereinafter referred to as Mekik et al., submitted manuscript, 2006], it is still empirical in nature and needs further corroboration from an independent calcite dissolution indicator. This is our main objective here. We choose Mg/Ca, Sr/Ca and Mg/Sr in deep dwelling planktonic foraminifer shells for comparison with MFI because *Brown and Elderfield* [1996], *Rosenthal et al.* [2000], *Rosenthal and Lohmann* [2002] and *Dekens et al.* [2002] established the potential of these element ratios as dissolution indicators. As foraminifer Mg/Ca has a strong temperature dependence, we restrict our study to a depth transect (1977–4441 m) on the Ontong Java Plateau (OJP) in order to minimize the variability in temperature (28.4–28.9°C) of our foraminifers' habitat waters and to isolate the effect of calcite dissolution on element ratios in foraminifer shells.

2.   Background
2.1.   *Globorotalia menardii* Fragmentation Index

[6] The *Globorotalia menardii* fragmentation index builds on *Ku and Oba*'s [1978] work and quantifies the amount of fragmentation of *G. menardii* shells in sediment. MFI is calculated as follows [after *Mekik et al.*, 2002]:

$$MFI = D/(D + W) \qquad (1)$$

where W is number of whole *G. menardii* specimens and D is (number of specimens with holes) plus (number greater than half intact) plus (number less than half/3) plus (keels/5). The choice of denominators for the various components in the calculation of D is based on averaged visual approximations of the number of fragments within a specific category needed to make up a complete *G. menardii* test. *Mekik et al.* [2002] derived a transfer function for calculating percent calcite dissolved from a regression between measured MFI values and percent calcite dissolved estimated with the biogeochemical model, Muds [*Archer et al.*, 2002] ($R^2 = 0.88$):

$$\% \text{ calcite dissolved} = -5.111 + (MFI * 160.491) \\ - (MFI^2 * 79.636) \qquad (2)$$

[7] Muds calculates calcite dissolution rates using seabed organic carbon flux ($\mu mol/cm^2/yr$), percent calcite in dry bulk

sediment, water depth (m) and bottom water $\Delta CO_3^=$ (= $[CO_3^=]$ of in situ seawater less $[CO_3^=]$ at calcite saturation, in $\mu mol/kg$). $\Delta CO_3^=$ at each site was obtained from *Archer*'s [1996; personal communication, 2001] global gridded database. Organic carbon fluxes were estimated from surface ocean productivity compilations of *Berger et al.* [1987], *Berger* [1989] and *Behrenfeld and Falkowski* [1997] and the attenuation of organic carbon flux with water depth (using *Berger et al.*'s [1987] equation). *Mekik et al.* [2002] also used *Jahnke*'s [1996] benthic oxygen flux data to independently estimate organic carbon fluxes for each sampling location. See *Mekik et al.* [2002] for further details on the modeling of percent calcite dissolved values used in the calibration of MFI.

[8] Core top calibration samples for MFI were chosen from depth transects on the OJP and the East Pacific Rise (EPR) outside of the upwelling region in order to isolate $\Delta CO_3^=$ as the dominant control on calcite dissolution and to minimize the variability in the rain ratio [*Mekik et al.*, 2002] which is more difficult to adequately constrain in the modern ocean [e.g., *Klaas and Archer*, 2002; *Mekik et al.*, 2002, 2006]. MFI's applicability in areas and oceanographic conditions beyond its calibration has been shown in subsequent studies, both in regions with variable seabed rain ratios [*Mekik et al.*, 2006] and in down core work [*Loubere et al.*, 2004; Mekik et al., submitted manuscript, 2006].

2.2.   Elemental Ratios in Planktonic Foraminifers

[9] Mg/Ca in foraminifer shells carries both a water temperature signal [*Nürnberg*, 1995; *Nürnberg et al.*, 1996; *Rosenthal et al.*, 1997; *Mashiotta et al.*, 1999; *Lea et al.*, 1999; *Elderfield and Ganssen*, 2000; *Lea et al.*, 2000; *Rosenthal and Lohmann*, 2002; *Dekens et al.*, 2002; *Lear et al.*, 2002; *Anand et al.*, 2003] and a calcite dissolution signal [*Brown and Elderfield*, 1996; *Rosenthal et al.*, 2000; *Dekens et al.*, 2002; *Rosenthal and Lohmann*, 2002]. The dissolution signal is easier to detect in shells of deeper dwelling species (such as *Neogloboquadrina dutertrei*), but is also present to some extent in shells of surface dwellers, such as *Globigerinoides ruber* and *Globigerinoides sacculifer* [*Dekens et al.*, 2002].

[10] *McCorkle et al.* [1995] reported a decrease of ∼15% in Sr/Ca in benthic foraminifers with increasing water depth below 2500 m on the OJP which they attributed to shell dissolution. *Brown and Elderfield* [1996] observed decreasing values of Sr/Ca in *G. tumida* with increasing water depth. They attributed this dissolution trend to chamber walls having higher Sr/Ca than keels, with the latter being more resistant to dissolution. *Elderfield et al.* [2000] also reported higher Sr/Ca in Globorotaliids in shallower water compared to those in deeper water. *Mortyn et al.* [2005] indicated that unlike non-Globorotaliids, Sr/Ca in Globorotaliids show significant variability from place to place. Thus we investigate Sr/Ca as a possible tracer of calcite dissolution in two Globorotaliid species: *G. menardii* and *G. tumida*.

3.   Methods
3.1.   Sampling Method

[11] We present new Mg/Ca, Mg/Sr and Sr/Ca data for several planktonic foraminifers from a subset of the same

Table 1. Core Information

Core	Latitude	Longitude	Water Depth, m	$\Delta CO_3^=$,[a] μmol/kg	T at 75 m,[b] °C	MFI Dissolved,[c] %
ERDC 98	−2.833	158.473	1977	−1.19	28.7	34.9
ERDC 116	−0.998	159.468	2272	−4.51	28.6	42.1
ERDC 118	−0.982	158.8	2163	−3.28	28.6	39.5
ERDC 121	−0.183	158.713	2245	−4.21	28.6	41.5
ERDC 126	−0.018	160.983	3328	−16.43	28.5	64.1
ERDC 127	−0.003	161.418	3724	−20.89	28.8	70.3
ERDC 130	−0.04	161.917	4123	−25.39	28.8	76.9
ERDC 132	−0.043	162.683	4441	−28.98	28.9	77.4
ERDC 90	−0.865	157.48	1903	−0.35	28.4	32.8
ERDC 89	−0.033	155.865	1932	−0.68	28.4	33.9
ERDC 115	−1.645	159.198	2157	−3.22	28.6	39.5
ERDC 109	−1.743	160.783	3636	−19.9	28	68.7
ERDC 110	−1.738	160.487	3003	−12.76	28.7	57.4
ERDC 111	−1.71	159.917	2667	−8.97	28.7	51.3
ERDC 114	−1.637	159.2	2151	−3.15	28.6	38

[a]Source is *Archer* [1996].
[b]Source is *Levitus and Boyer* [1994].
[c]Source is *Mekik et al.* [2002].

core top samples with which MFI was originally calibrated. In order to limit temperature variability among samples, we limited our sampling to MFI's calibration samples from the OJP only (Table 1). All samples are from gravity cores.

[12] Considering that deep dwelling planktonic foraminifers are subject to a smaller range of temperatures than surface dwellers and that their elemental ratios may be more sensitive to calcite dissolution, we chose deep dwellers to better isolate the dissolution signal recorded in their shell chemistry. According to *Anand et al.* [2003], *N. dutertrei* and *Pulleniatina obliquiloculata* live at 50–100 m water depth. According to *Schweitzer and Lohmann* [1991], *Globorotalia tumida*s grow their chambers above 50 m but their keels between 50–100 m. *G. menardii*s are known to have symbionts, so they spend part of their life cycle close to the surface but are mostly thermocline dwellers [*Bé*, 1960].

[13] Foraminifers were picked individually in a given size range for each species, and all the picking was done by the same person (F. Mekik). *N. dutertrei* was picked from a 400–500 μm size range, *P. obliquiloculata* from 420–510 μm, *G. menardii* from 700–800 μm and *G. tumida* from 900–1000 μm. These size ranges (within ∼100 μm) are similar to those used by *Brown and Elderfield* [1996]

and *Dekens et al.* [2002], but our specimens are somewhat larger. Our results might have been more reproducible had we been able to find a sufficient number of foraminifers in a narrower size range [*Elderfield et al.*, 2002]. On the other hand, the comparatively larger size of our specimens may have increased our precision, since analytical reproducibility appears to increase with increasing foraminifer shell size (J. Bijma, personal communication, 2006).

3.2. Sample Preparation

[14] Samples were prepared using the *Barker et al.* [2003] cleaning protocol because it has been shown that more rigorous cleaning with a reductive step causes dissolution of planktonic foraminifer test material and biases results [*Rosenthal et al.*, 2004]. However, we modified this cleaning protocol in two ways: (1) by using a scalpel to cut each foraminifer into two under the microscope instead of breaking foraminifers between glass plates, minimizing sample loss during cleaning and also ensuring that foreign particles are completely removed from each chamber, and (2) by adding a 5-min centrifuging step between each rinse with H_2O_2 to collect foraminifers at the bottom of the tubes and to minimize sample loss during cleaning.

Table 2. Number of Foraminifers in Each Measurement

Core	*N. dutertrei* Measured	Duplicate	*G. menardii* Measured	Duplicate	*P. obliquiloculata* Measured	Duplicate	*G. tumida* Measured	Duplicate
ERDC 98	22	7	4		40	24		
ERDC 116	20				25	28	9	
ERDC 118	10		6				8	
ERDC 121							8	
ERDC 126					26	19	7	
ERDC 127			7	4	43	27	9	10
ERDC 130			5				4	
ERDC 132			4		35	13	14	
ERDC 90			8		34	26		
ERDC 89	25	4	11		30	17		
ERDC 115	13	6			27	22	5	
ERDC 109					33	28	6	6
ERDC 110					31		5	
ERDC 111					27		6	
ERDC 114			5	5	14		2	

Table 3. Element Ratio Data[a]

Core	N. dutertrei Measured	N. dutertrei Duplicate	G. menardii Measured	G. menardii Duplicate	P. obliquiloculata Measured	P. obliquiloculata Duplicate	G. tumida Measured	G. tumida Duplicate
				Mg/Ca				
ERDC 98	2.95 ± 0.17	2.9 ± 0.17	2.53 ± 0.17		2.59 ± 0.15	2.73 ± 0.16		
ERDC 116	2.16 ± 0.16				2.57 ± 0.15	2.76 ± 0.16	1.75 ± 0.1	
ERDC 118	2.37 ± 0.14		2.26 ± 0.12				2.34 ± 0.13	
ERDC 121							1.98 ± 0.18	
ERDC 126					2.44 ± 0.14	2.47 ± 0.14	1.91 ±0.11	
ERDC 127			1.4 ± 0.09	1.2 ± 0.09	2.24 ± 0.16	2.07 ± 0.12	1.56 ± 0.11	1.57 ± 0.09
ERDC 130			1.66 ± 0.17				1.4 ± 0.15	
ERDC 132			1.46 ± 0.09		1.94 ± 0.12	1.69 ± 0.11	1.32 ±0.13	
ERDC 90			2.41 ± 0.24		2.67 ± 0.2	2.75 ± 0.17		
ERDC 89	2.36 ± 0.23	2.31 ± 0.23	2.46 ± 0.16		3.05 ± 0.19	2.97 ± 0.17		
ERDC 115	2.73 ± 0.28				2.64 ± 0.22	2.84 ± 0.17	2.1 ± 0.15	
ERDC 109					2.21 ± 0.14	2.3 ± 0.14	1.6 ± 0.13	1.79 ± 0.11
ERDC 110					2.57 ± 0.23		2.15 ± 0.21	
ERDC 111					2.66 ± 0.15		2.05 ± 0.17	
ERDC 114			2.68 ± 0.22	2.66 ± 0.16	2.64 ± 0.15		2.83 ±0.23	
				Sr/Ca				
ERDC 98	1.08 ± 0.05		1 ± 0.04		1.26 ± 0.05	1.48 ± 0.06		
ERDC 116	1.05 ± 0.05				1.26 ± 0.05	1.55 ± 0.06	1.12 ± 0.05	
ERDC 118	1.21 ± 0.05		1.16 ± 0.05				1.13 ± 0.05	
ERDC 121					1.32 ± 0.08		1.15 ± 0.08	
ERDC 126					1.25 ± 0.05	1.4 ± 0.06	1.12 ± 0.05	
ERDC 127			1.14 ± 0.05	1.2 ± 0.05	1.28 ± 0.08	1.39 ± 0.06	1.08 ± 0.07	1.26 ± 0.05
ERDC 130			1.13 ± 0.07		1.41 ± 0.08	1.48 ± 0.06	1.18 ± 0.09	
ERDC 132			1.21 ± 0.05		1.3 ± 0.06	1.31 ± 0.06	1.13 ± 0.07	
ERDC 90			1.15 ± 0.08		1.24 ± 0.08	1.45 ± 0.06		
ERDC 89	1.29 ± 0.09	1.3 ± 0.01	1.21 ± 0.06		1.33 ± 0.06			
ERDC 115	1.24 ± 0.08	1.28 ± 0.05			1.33 ± 0.09	1.52 ± 0.06	1.15 ± 0.06	
ERDC 109					1.29 ± 0.11	1.44 ± 0.06	1.15 ± 0.08	1.29 ± 0.05
ERDC 110					1.3 ± 0.09		1.2 ± 0.08	
ERDC 111					1.44 ± 0.06		1.16 ± 0.07	
ERDC 114			1.16 ± 0.08		1.49 ± 0.06		1.06 ± 0.06	
				Mg/Sr				
ERDC 98	2.73 ± 0.16		2.53 ± 0.20		2.06 ± 0.13	1.84 ± 0.11		
ERDC 116	2.06 ± 0.17				2.04 ± 0.13	1.78 ± 0.11	1.55 ± 0.10	
ERDC 118	1.96 ± 0.14		1.95 ± 0.13				2.11 ± 0.14	
ERDC 121							1.72 ± 0.17	
ERDC 126					1.95 ± 0.12	1.76 ± 0.11	1.71 ± 0.12	
ERDC 127			1.23 ± 0.08	1 ± 0.08	1.75 ± 0.12	1.49 ± 0.09	1.44 ± 0.10	1.25 ± 0.09
ERDC 130			1.47 ± 0.14				1.19 ± 0.12	
ERDC 132			1.21 ± 0.08		1.49 ± 0.10	1.29 ± 0.09	1.17 ± 0.10	
ERDC 90			2.09 ± 0.20		2.15 ± 0.14	1.9 ± 0.10		
ERDC 89	1.82 ± 0.18	1.78 ± 0.18	2.03 ± 0.15		2.29 ± 0.15			
ERDC 115	2.22 ± 0.23				1.98 ± 0.15	1.87 ± 0.12	1.83 ± 0.14	
ERDC 109					1.71 ± 0.19	1.6 ± 0.10	1.39 ± 0.11	1.39 ± 0.11
ERDC 110					1.98 ± 0.18		1.79 ± 0.17	
ERDC 111					1.85 ± 0.11		1.65 ± 0.13	
ERDC 114			2.31 ± 0.17	1.94 ± 0.09	1.75 ± 0.11		2.67 ± 0.23	

[a]Values are given in mmol/mol for Mg/Ca and Sr/Ca and mmol/mmol for Mg/Sr.

3.3. Analytical Method

[15] The Element 2 Inductively Coupled Plasma Mass Spectrometer (ICP-MS) at the University of British Columbia (Vancouver, British Columbia) was used for the simultaneous determination of Mg/Ca, Sr/Ca and Mg/Sr from our foraminifer samples following the method described by *Rosenthal et al.* [1999]. Standard solutions were prepared gravimetrically: a set for Mg and Sr and another set for Ca alone. All standard and sample solutions were made with 0.075M nitric acid. ^{43}Ca was measured to determine Ca concentrations in all our standards and samples. Polyatomic interferences on Ca and matrix effects on elemental ratios are insignificant in the concentration range used in our analyses [*Rosenthal et al.*, 1999].

[16] We report Mg/Ca and Sr/Ca in *N. dutertrei, P. obliquiloculata, G. menardii* and *G. tumida* shells. Table 2 lists the number of foraminifers used for each measurement and Table 3 lists elemental ratios, duplicate measurements and the analytical error associated with each measurement. Analytical errors (66% confidence interval) are calculated from counting statistics for the ratio of each element to our internal standard (indium) and the uncertainties on the intercept and slope of the linear regressions obtained with our standard solutions. Duplicate measurements were made
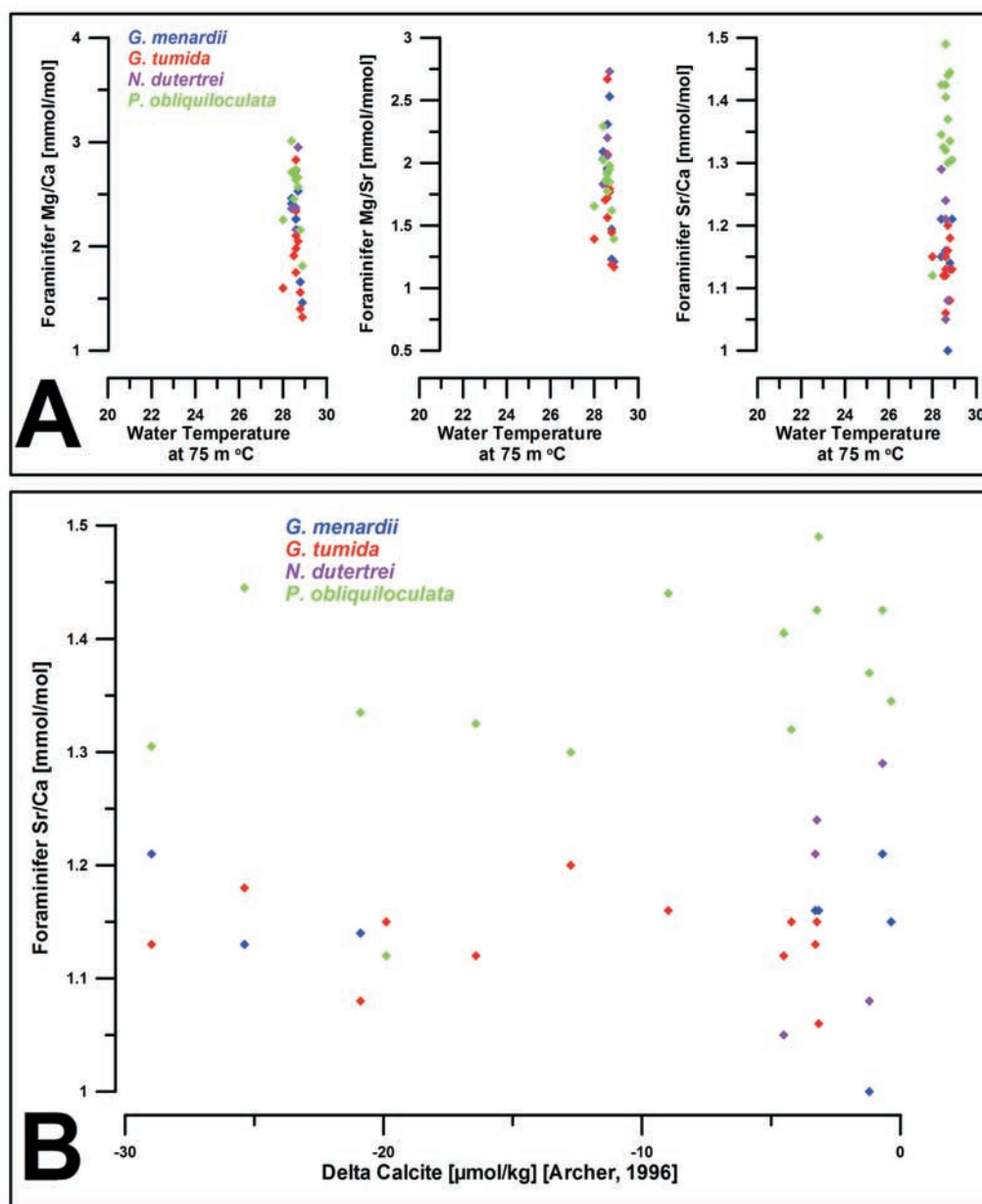
Figure 1. (a) Temperature at 75 m water depth [*Levitus and Boyer*, 1994] plotted against foraminifer Mg/Ca, Mg/Sr, and Sr/Ca. (b) $\Delta CO_3^=$ [*Archer*, 1996] plotted against foraminifer Sr/Ca. All samples are from the Ontong Java Plateau.

on a subset of our samples where enough foraminifer material was available (Table 3).

4. Results

[17] Figure 1a shows the Mg/Ca, Mg/Sr and Sr/Ca ratios of foraminifers plotted against water temperature at 75 m depth [from *Levitus and Boyer*, 1994]. The effect of temperature variability must be minimal on Mg/Ca measurements in our samples from the OJP because all our sampling locations fall within a tight temperature range at the mean habitat depths of the foraminifer species under consideration (~75 m). All foraminifer samples have a large

range of variability in Mg/Ca, Mg/Sr and Sr/Ca at similar temperatures on the OJP (Figure 1a).

[18] Figure 1b shows the relationship of Sr/Ca in each of our species with $\Delta CO_3^=$ from *Archer*'s [1996] global gridded database. Although *Elderfield et al.* [2000] found a decrease in Sr/Ca with water depth in *G. tumida*, we find no relationship in our samples between any of our foraminifers' Sr/Ca and $\Delta CO_3^=$, including *G. tumida*. This may not be surprising since Sr appears to be homogeneously distributed throughout most foraminifer shells [*Bender et al.*, 1975]. However, the discrepancy between *Elderfield et al.*'s [2000] results and ours remains
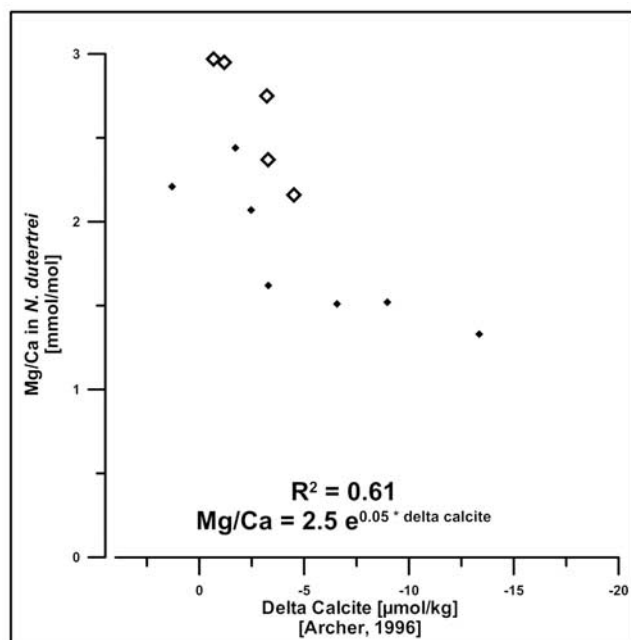
Figure 2. Plot of $\Delta CO_3^=$ against Mg/Ca in *N. dutertrei*. Solid diamonds show data from *Dekens et al.* [2002] (250–350 μm). Open diamonds show new data (400–500 μm). Samples are from the Ontong Java Plateau.

unexplained. Since Sr also appears to be homogeneous in our foraminifers, we investigated a dissolution trend using Mg/Sr as well as Mg/Ca.

[19] Our *N. dutertrei* samples are limited in number and in their range of $\Delta CO_3^=$. We therefore complemented them with a subset of *Dekens et al.*'s [2002] Mg/Ca data set. We show a subset of the data from *Dekens et al.*'s [2002] corresponding to the MFI calibration sites on the OJP to minimize temperature variability among samples. The open symbols correspond to our Mg/Ca data. Note that *Dekens et al.* [2002] used a 250–350 μm size range for *N. dutertrei*, while we used 400–500 μm. The trend of our data seems to mesh moderately well with theirs when plotted against $\Delta CO_3^=$ (values from *Archer* [1996]) ($R^2 = 0.61$) (Figure 2). The relationship between Mg/Ca in *N. dutertrei* and $\Delta CO_3^=$ would likely be stronger had we used *N. dutertrei* tests of the same size as those used by *Dekens et al.* [2002].

[20] In Figure 3, we present Mg/Ca and Mg/Sr in *G. menardii, P. obliquiloculata* and *G. tumida* plotted against $\Delta CO_3^=$. There is a clear decrease in Mg/Ca in both *G. menardii* and *P. obliquiloculata* with increasingly negative $\Delta CO_3^=$ ($R^2 = 0.87 – 0.88$); and a similar but somewhat lower correlation between Mg/Sr and $\Delta CO_3^=$ ($R^2 = 0.68 – 0.82$). These relationships in *G. tumida* are less robust ($R^2 = 0.64 – 0.71$) and better fitted with an exponential curve, suggesting that changes in elemental ratios in this species may be more sensitive to the low end of calcite dissolution.

[21] Figure 4 shows the same data plotted against model-derived estimates of percent calcite dissolved per sample location. The relationship between Mg/Ca or Mg/Sr and

modeled percent calcite dissolved is statistically similar to those with $\Delta CO_3^=$ (Figure 3). Thus we are able to illustrate that there is a good linear trend between geochemical measurements from foraminifer shells and both modeled estimates of percent calcite dissolved and $\Delta CO_3^=$.

[22] Plotting Mg/Ca and Mg/Sr from the three foraminifer species against the fragmentation trend of *G. menardii* (MFI) in the same sediment samples (Figure 5) and against percent calcite dissolved using the MFI transfer function of *Mekik et al.* [2002] (Figure 6) reveals equally strong relationships for *G. menardii* and *P. obliquiloculata* ($R^2 = 0.74 – 0.94$ for MFI; $R^2 = 0.69 – 0.88$ for percent dissolved). Again, the relationships with *G. tumida* are less robust ($R^2 = 0.64 – 0.69$ for MFI; $R^2 = 0.58 – 0.63$ for percent dissolved).

5. Discussion

[23] Our data indicate that both MFI and elemental ratios from our deep dwelling foraminifer species, Mg/Ca and Mg/Sr, covary in response to decreasing $\Delta CO_3^=$ and increasing calcite dissolution in the sediments. Other element/Ca ratios from foraminifer shells have been shown to also decrease with increasing dissolution, such as F/Ca [*Rosenthal and Boyle*, 1993], V/Ca [*Hastings*, 1994] and U/Ca [*Russell*, 1994]. Since we carefully chose our samples so as to limit the effect of temperature and other possible confounding variables (such as surface water [$CO_3^=$] and nutrient concentration) on foraminifer elemental ratios, this finding provides independent corroboration for MFI as a dissolution proxy.

[24] The prospect of using foraminifer Mg/Ca as a calcite dissolution indicator is hindered by its strong temperature dependence in foraminifer shells [*Nürnberg*, 1995; *Nürnberg et al.*, 1996; *Rosenthal et al.*, 1997; *Mashiotta et al.*, 1999; *Lea et al.*, 1999; *Elderfield and Ganssen*, 2000; *Lea et al.*, 2000; *Rosenthal and Lohmann*, 2002; *Dekens et al.*, 2002; *Lear et al.*, 2002; *Anand et al.*, 2003]. Foraminifer Mg/Ca from samples with similar MFI values but collected over a wider range of temperature would establish the temperature dependence of Mg/Ca in *P. obliquiloculata*, *G. menardii* and *G. tumida*. This temperature signal combined with independent estimates of water temperature at their habitat depths could then be used to estimate down core variations in calcite dissolution from Mg/Ca in deep dwellers, although finding appropriate temperature proxies for such a purpose may prove difficult. Alternatively, if we can confirm and more precisely constrain the correlation between dissolution induced changes in Mg/Ca from deep dwelling foraminifers and MFI that we have documented in this study, we could combine these two measurements in down core samples to assess past changes in subsurface seawater temperature.

[25] As $\Delta CO_3^=$ decreases from 0 to -30 μmol/kg, there is a $\sim$55% drop in Mg/Ca and Mg/Sr of *G. tumida*; $\sim$50% drop in *G. menardii*; and a $\sim$30% drop in *P. obliquiloculata* Mg/Ca and Mg/Sr. This $\Delta CO_3^=$ range corresponds to an increase in modeled percent calcite dissolved from 45%–80%. A closer examination of Figures 3 through 6 suggests that elemental ratios in *P. obliquiloculata* may be more sensitive to percent dissolved less than 50%, while elemental ratios in *G. tumida*
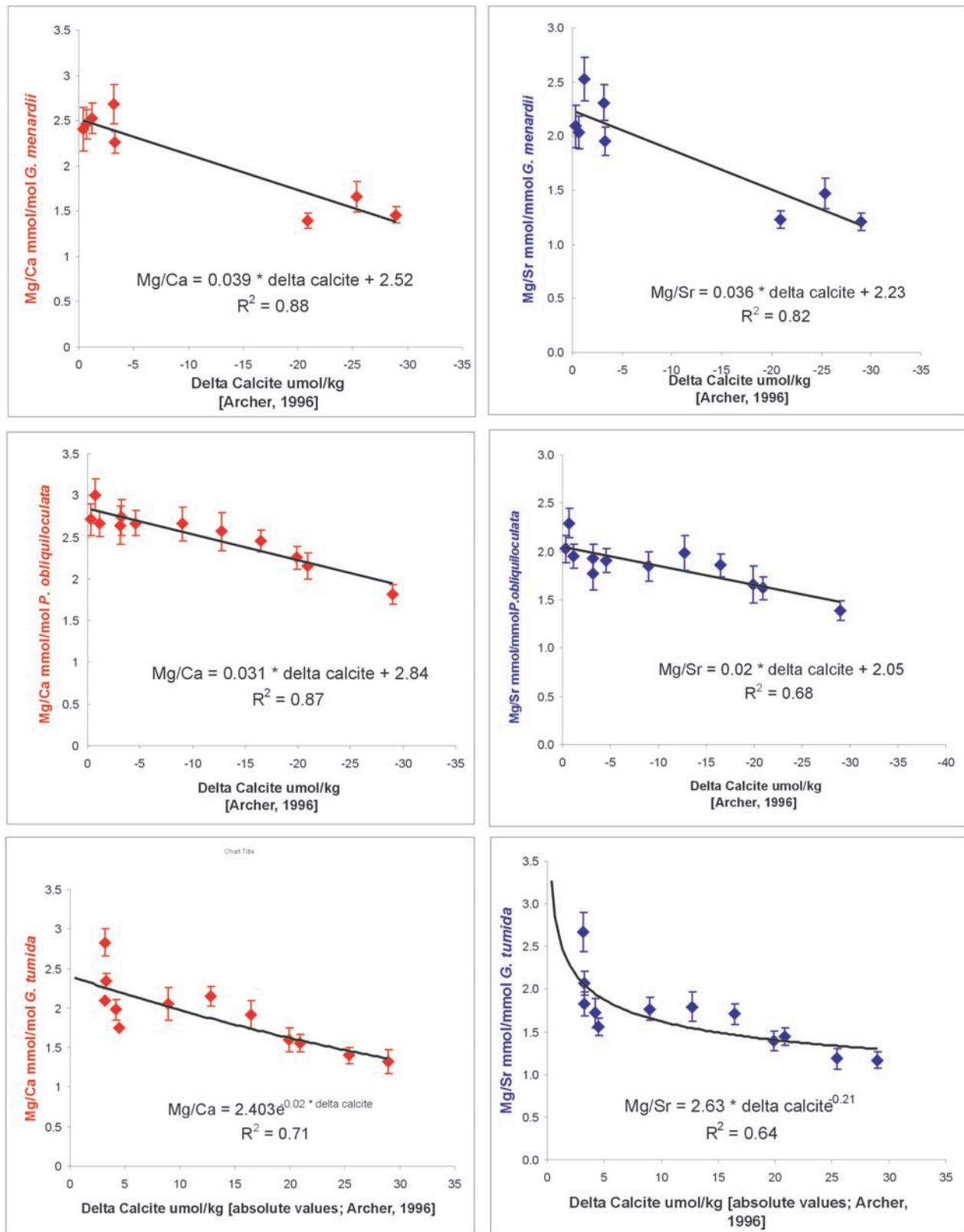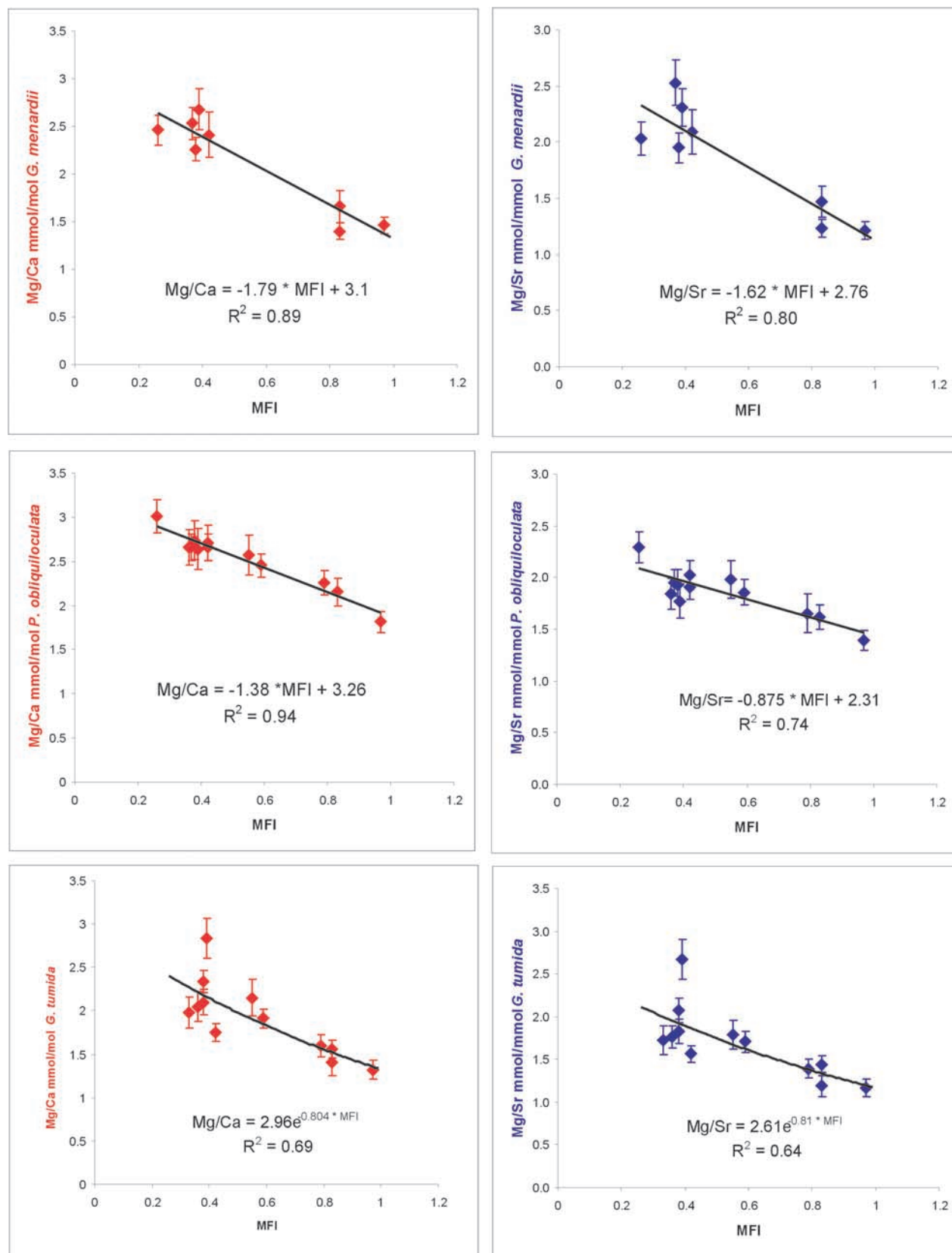
Figure 3. $\Delta CO_3^=$ plotted against foraminifer Mg/Ca and Mg/Sr data. Bars show analytical error margins as listed in Table 3. Samples are from the Ontong Java Plateau.
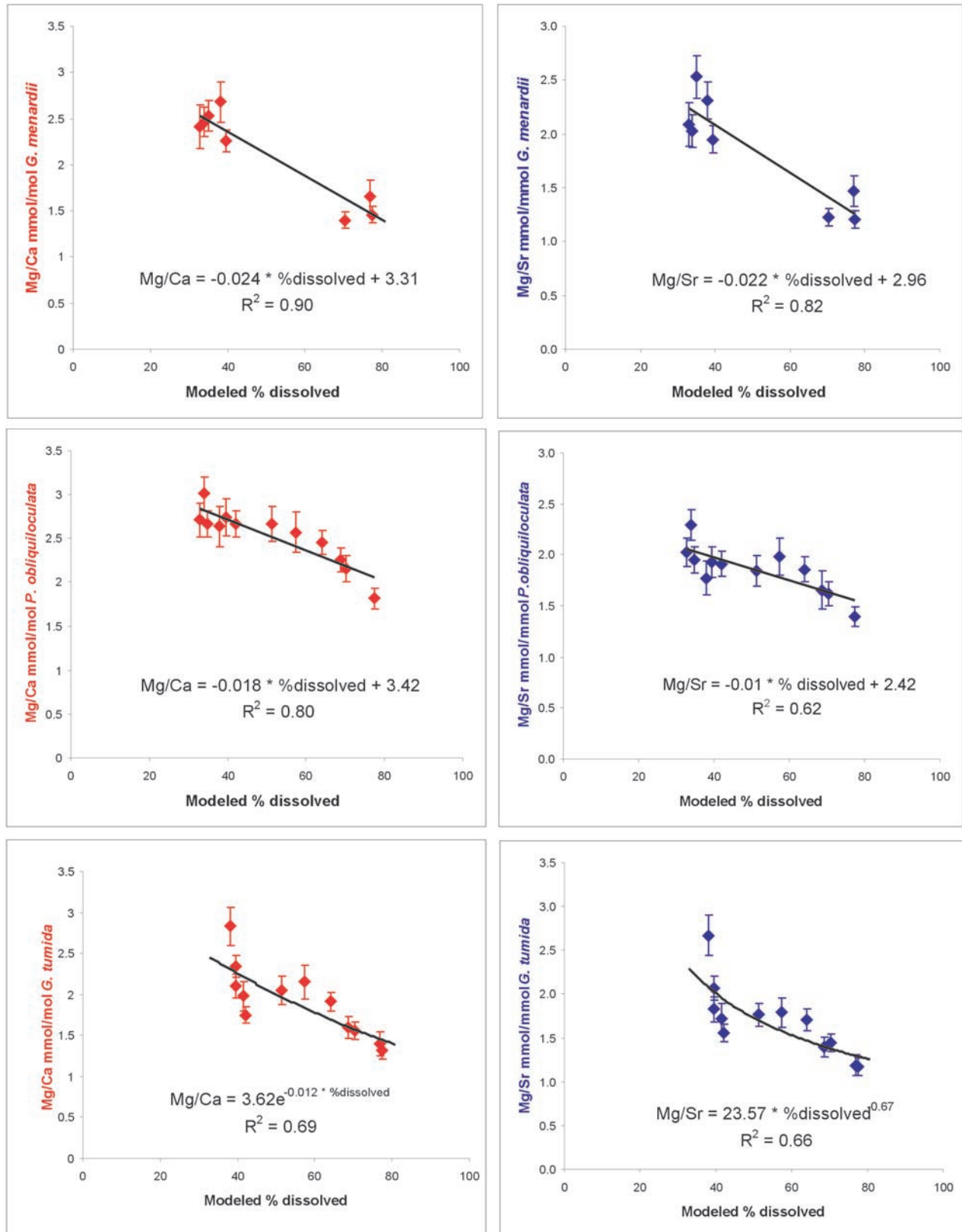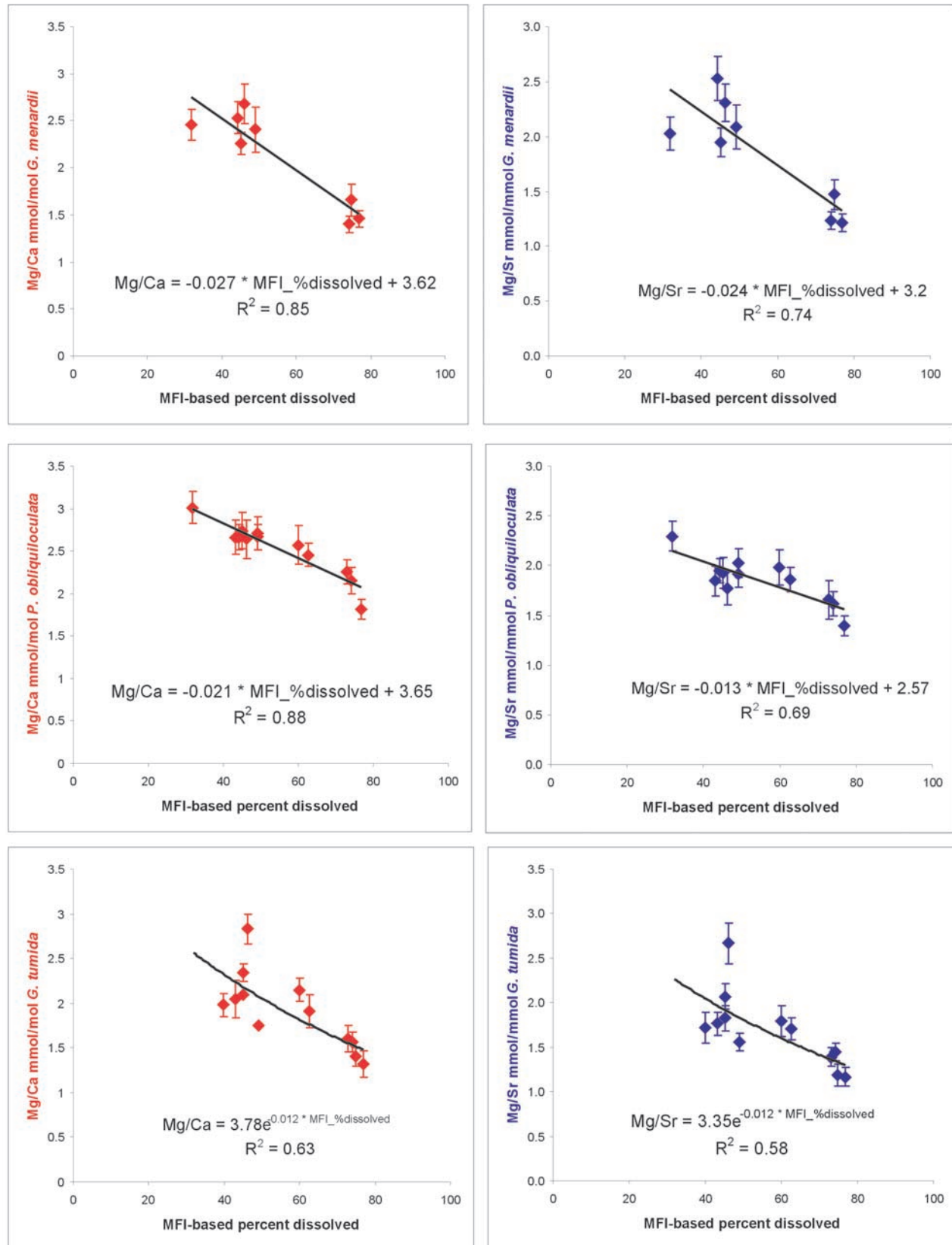
Figure 4. Modeled estimates of percent calcite dissolved plotted against foraminifer Mg/Ca and Mg/Sr data. Bars show analytical error margins as listed in Table 3. Samples are from the Ontong Java Plateau.

Figure 5. MFI plotted against foraminifer Mg/Ca and Mg/Sr data. Bars show analytical error margins as listed in Table 3. Samples are from the Ontong Java Plateau.

MEKIK AND FRANÇOIS: DEEP-SEA CARBONATE DISSOLUTION

Figure 6. Estimates of percent calcite dissolved with the MFI transfer function [*Mekik et al.*, 2002] plotted against foraminifer Mg/Ca and Mg/Sr data. Bars show analytical error margins as listed in Table 3. Samples are from the Ontong Java Plateau.

may be more sensitive to percent dissolved greater than 50%. If confirmed, such trends would point to combining the analysis of different species of foraminifers to optimally reconstruct calcite dissolution over the entire water depth range.

[26] *Dekens et al.* [2002] showed that Mg/Ca in deep dwelling foraminifers (*N. dutertrei* in their work) is more susceptible to dissolution than Mg/Ca in surface dwellers. Surface dwellers (e.g., *G. ruber* and *G. sacculifer*) thus appear to be better suited to record sea surface temperature (SST) variations. *Dekens et al.* [2002] also state that though Mg/Ca from *G. ruber* and *G. sacculifer* primarily carry a temperature signal, they also have a $\Delta CO_3^=$ overprint, though to a lesser degree than Mg/Ca from *N. dutertrei*. Since the temperature dependence of Mg/Ca in *G. ruber* and *G. sacculifer* has been well established [e.g., *Lea et al.*, 2000; *Dekens et al.*, 2002; *Rosenthal and Lohmann*, 2002], it may be possible to tease out the effect of calcite dissolution on the Mg/Ca of these two surface dwellers (as we have done with other species herein) by analyzing samples representing a wide range of calcite dissolution but limited temperature variability. If a correlation between dissolution induced changes in the elemental ratios of surface dwellers and MFI can be found, then down core Mg/Ca–derived SST reconstructions could be corrected for calcite dissolution in areas where foraminifer material for both proxies (Mg/Ca and MFI) are available in the same cores.

6. Conclusions

[27] We compared a foraminifer fragmentation proxy (*G. menardii* fragmentation index (MFI)) with elemental ratios from foraminifer shells in the same samples. Our sample locations were carefully chosen so as to provide sediment samples subjected to a wide range of seabed calcite dissolution and surface water conditions with a narrow range of temperature, $[CO_3^=]$ and nutrient concentrations. We studied deep dwelling planktonic foraminifers based on the work of *Dekens et al.* [2002] which indicated that deeper water foraminifers are more sensitive to dissolution than are surface dwellers. The correlations between MFI, elemental ratios, modeled percent calcite dissolved and $\Delta CO_3^=$ lend support for the use of MFI as a reliable calcite dissolution proxy. Mg/Ca or Mg/Sr in *P. obliquiloculata, G. menardii* and possibly *G. tumida* would also have the potential for use as calcite dissolution indicators after the temperature dependence of their signal is established. Alternatively, combining Mg/Ca in deep dwelling foraminifers with MFI, could provide a means for accurately estimating past changes in water temperature at these foraminifers' habitat depths. Likewise, finding a correlation between dissolution-induced changes in the elemental ratios of surface dwellers and MFI could provide a tool to correct sea surface temperature estimates for calcite dissolution.

References

Anand, P., H. Elderfield, and M. H. Conte (2003), Calibration of Mg/Ca thermometry in planktonic foraminifera from a sediment trap time series, *Paleoceanography*, *18*(2), 1050, doi:10.1029/2002PA000846.

Archer, D. E. (1996), An atlas of the distribution of calcium calcite in sediments of the deep sea, *Global Biogeochem. Cycles*, *10*, 159–174.

Archer, D., and E. Maier-Reimer (1994), Effect of deep sea sedimentary calcite preservation on atmospheric CO_2 concentration, *Nature*, *367*, 260–264.

Archer, D. E., J. L. Morford, and S. Emerson (2002), A model of suboxic sedimentary diagenesis suitable for automatic tuning and gridded global domains, *Global Biogeochem. Cycles*, *16*(1), 1017, doi:10.1029/2000GB001288.

Arrhenius, G. (1952), Sediment cores from the east Pacific, *Rep. Swed. Deep Sea Exped. 1947–1948*, *5*, 1–228.

Barker, S., M. Greaves, and H. Elderfield (2003), A study of cleaning procedures used for foraminiferal Mg/Ca paleothermometry, *Geochem. Geophys. Geosyst.*, *4*(9), 8407, doi:10.1029/2003GC000559.

Bé, A. W. H. (1960), Ecology of Recent planktonic foraminifera: part 2–Bathymetric and seasonal distributions in the Sargasso Sea off Bermuda, *Micropaleontology*, *6*, 373–392.

Behrenfeld, M., and P. Falkowski (1997), Photosynthetic rates derived from satellite based chlorophyll concentration, *Limnology Oceanogr.*, *42*, 1–20.

Bender, M. L., R. B. Lorenz, and D. F. Williams (1975), Sodium, magnesium and strontium in the tests of planktonic foraminifera, *Micropaleontology*, *21*, 448–459.

Berger, W. (1968), Planktonic foraminifera: Selective solution and paleoclimatic interpretation, *Deep Sea Res. Oceanogr. Abstr.*, *15*, 31–43.

Berger, W. (1970), Planktonic foraminifera: Selective solution and the lysocline, *Mar. Geol.*, *8*, 111–138.

Berger, W. (1975), Deep sea calcites: Dissolution profiles from foraminiferal preservation, in *Dissolution of Deep Sea Calcites*, vol. 13, edited by E. W. H. Be and W. H. Berger, pp. 82–86, Spec. Publ. Cushman Found. Foraminiferal Res., Washington D. C.

Berger, W. (1989), Global maps of ocean productivity, in *Productivity of the Ocean: Present and Past*, edited by W. H. Berger, V. S. Smetacek, and G. Wefer, pp. 429–455, John Wiley, Hoboken, N. J.

Berger, W., K. Fischer, C. Cai, and G. Wu (1987), Organic productivity and organic carbon flux, I, in *Overview and Maps of Primary Production and Export Production, Rep. 87–30*, pp. 1–45, Scripps Inst. of Oceanogr., Univ. of California, La Jolla.

Broecker, W. S., and E. Clark (1999), Calcite size fractions: A paleocalcite ion proxy, *Paleoceanography*, *14*, 596–604.

Broecker, W. S., and E. Clark (2001), An evaluation of Lohmann's foraminifera weight dissolution index, *Paleoceanography*, *16*, 431–434.

Brown, S. J., and H. Elderfield (1996), Variations in Mg/Ca and Sr/Ca ratios of planktonic foraminifera caused by post-depositional dissolution, *Paleoceanography*, *11*, 543–551.

Dekens, P. S., D. W. Lea, D. K. Pak, and H. J. Spero (2002), Core top calibration of Mg/Ca in tropical foraminifera: Refining paleotemperature estimation, *Geochem. Geophys. Geosyst.*, *3*(4), 1022, doi:10.1029/2001GC000200.

Elderfield, H., and G. Ganssen (2000), Reconstruction of temperature and $\delta^{18}O$ of surface

ocean waters using Mg/Ca of planktonic for-aminiferal calcite, *Nature*, *405*, 442–445.

Elderfield, H., M. Cooper, and G. Ganssen (2000), Sr/Ca in multiple species of planktonic foraminifera: Implications for reconstructions of seawater Sr/Ca, *Geochem. Geophys. Geosyst.*, *1*(11), doi:10.1029/1999GC000031.

Elderfield, H., M. Vautravers, and M. Cooper (2002), The relationship between shell size and Mg/Ca, Sr/Ca δ¹⁸O and δ¹³C of species of planktonic foraminifera, *Geochem. Geophys. Geosyst.*, *3*(8), 1052, doi:10.1029/2001GC000194.

Emerson, S., and M. Bender (1981), Carbon fluxes at the sediment-water interface of the deep sea: Calcium carbonate preservation, *J. Mar. Res.*, *39*, 139–162.

Hastings, D. W. (1994), Vanadium in the ocean: A marine mass balance and paleoseawater record, Ph.D. dissertation, Univ. of Wash., Seattle.

Jahnke, R. A. (1996), The global ocean flux of particulate organic carbon: Areal distribution and magnitude, *Global Biogeochem. Cycles*, *10*, 71–88.

Klaas, C., and D. Archer (2002), Association of sinking organic matter with various types of mineral ballast in the deep sea: Implications for the rain ratio, *Global Biogeochem. Cycles*, *16*(4), 1116, doi:10.1029/2001GB001765.

Ku, T.-L., and T. Oba (1978), A method of quantitative evaluation of calcite dissolution in deep sea sediments and its application to paleoceanographic reconstruction, *Quat. Res.*, *10*, 112–129.

Le, J., and N. J. Shackleton (1992), Carbonate dissolution fluctuations in the western equatorial Pacific during the late Quaternary, *Paleoceanography*, *7*, 21–42.

Lea, D. W., T. A. Mashiotta, and H. J. Spero (1999), Controls on magnesium and strontium uptake in planktonic foraminifera determined by live culturing, *Geochim., Cosmochim. Acta*, *63*, 2369–2379.

Lea, D. W., D. K. Pak, and H. J. Spero (2000), Climatic impact of the late Quaternary equatorial Pacific sea surface temperature, *Science*, *289*, 1719–1724.

Lear, C. H., Y. Rosenthal, and N. Slowey (2002), Benthic foraminiferal Mg/Ca paleothermometry: A revised core top calibration, *Geochim. Cosmochim. Acta*, *66*, 3375–3387.

Levitus, S., and T. P. Boyer (1994), *World Ocean Atlas 1994*, vol. 4, *Temperature*, NOAA Atlas NESDIS, vol. 4, 129 pp., NOAA, Silver Spring, Md.

Lohmann, G. P. (1995), A model for variation in the chemistry of planktonic foraminifera due to secondary calcification and selective dissolution, *Paleoceanography*, *10*(3), 445–457.

Loubere, P., F. A. Mekik, R. François, and S. Pichat (2004), Export fluxes of calcite in the eastern equatorial Pacific from the Last Glacial Maximum to Present, *Paleoceanography*, *19*, PA2018, doi:10.1029/2003PA000986.

Mashiotta, T. A., D. W. Lea, and H. J. Spero (1999), Glacial-interglacial changes in subantarctic sea surface temperature and δ¹⁸O-water using foraminiferal Mg, *Earth Planet. Sci. Lett.*, *170*, 417–432.

McCorkle, D., P. Martin, D. W. Lea, and G. P. Klinkhammer (1995), Evidence of a dissolution effect on benthic foraminiferal shell chemistry: δ¹³C, Cd/Ca, Ba/Ca, and Sr/Ca results from the Ontong Java Plateau, *Paleoceanography*, *10*, 699–714.

Mekik, F. A., P. Loubere, and D. Archer (2002), Organic carbon flux and organic carbon to calcite flux ratio recorded in deep sea calcites: Demonstration and a new proxy, *Global Biogeochem. Cycles*, *16*(3), 1052, doi:10.1029/2001GB001634.

Mekik, F. A., P. Loubere, and M. Richaud (2006), Rain ratio variation in the tropical ocean: Tests with surface sediments in the eastern equatorial Pacific, *Deep Sea Res. Part II*, in press.

Mortyn, P. G., H. Elderfield, P. Anand, and M. Greaves (2005), An evaluation of controls on planktonic foraminiferal Sr/Ca: Comparison of water column and core-top data from a North Atlantic transect, *Geochem. Geophys. Geosyst.*, *6*, Q12007, doi:10.1029/2005GC001047.

Nürnberg, D. (1995), Magnesium in tests of *Neogloboquadrina pachyderma* sinistral from high northern and southern latitudes, *J. Foraminiferal Res.*, *25*, 350–368.

Nürnberg, D., J. Bijma, and C. Hemleben (1996), Assessing the reliability of magnesium in foraminiferal calcite as a proxy for water mass temperatures, *Geochim. Cosmochim. Acta*, *60*, 803–814.

Oba, T. (1969), Biostratigraphy and isotopic paleo-temperature of some deep sea cores from the Indian Ocean, *Second Ser. Sci. Rep. 41*, pp. 129–195, Tohoku Univ., Sendai, Japan.

Peterson, L. P., and W. C. Prell (1985a), Calcite dissolution in recent sediments of the eastern equatorial Indian Ocean: Preservation patterns and calcite loss above the lysocline, *Mar. Geol.*, *64*, 259–290.

Peterson, L. P., and W. C. Prell, (1985b), Calcite preservation and rates of climatic change: An 800 kyr record from the Indian Ocean, in *The Carbon Cycle and Atmospheric CO₂: Natural Variations Archean to Present, Geophys. Monograph Ser.*, vol. 32, edited by E. T. Sundquist and W. S.

Broecker, pp. 251–269, AGU, Washington, D. C.

Rosenthal, Y., and E. A. Boyle (1993), Factors controlling the fluoride content of planktonic foraminifera: An evaluation of its paleoceanographic applicability, *Geochim. Cosmochim. Acta*, *57*, 335–346.

Rosenthal, Y., and G. P. Lohmann (2002), Accurate estimation of sea surface temperatures using dissolution-corrected calibrations for Mg/Ca paleo-thermometry, *Paleoceanography*, *17*(3), 1044, doi:10.1029/2001PA000749.

Rosenthal, Y., E. A. Boyle, and N. Slowey (1997), Environmental controls on the incorporation of Mg, Sr, F and Cd into benthic foraminifera shells from Little Bahama Bank: Prospects for thermocline paleoceanography, *Geochim. Cosmochim. Acta*, *61*, 3633–3643.

Rosenthal, Y., P. M. Field, and R. M. Sherrell (1999), Precise determination of element/calcium ratios in calcareous samples using sector field inductively coupled plasma mass spectrometry, *Anal. Chem.*, *71*, 3248–3253.

Rosenthal, Y., G. P. Lohmann, K. C. Lohmann, and R. M. Sherrell (2000), Incorporation and preservation of Mg in *G. sacculifer*: Implications for reconstructing sea surface temperatures and the oxygen isotopic composition of sea water, *Paleoceanography*, *15*, 135–145.

Rosenthal, Y., et al. (2004), Interlaboratory comparison study of Mg/Ca and Sr/Ca measurements in planktonic foraminifera for paleoceanographic research, *Geochem. Geophys. Geosyst.*, *5*, Q04D09, doi:10.1029/2003GC000650.

Russell, A. D. (1994), Uranium in foraminiferal calcite: Incorporation, preservation and seawater record, Ph.D. dissertation, Univ. of Washington, Seattle.

Schweitzer, P. N., and G. P. Lohmann (1991), Ontogeny and habitat of modern menardii form planktonic foraminifera, *J. Foraminiferal Res.*, *21*(4), 332–346.

Thompson, P. R., and T. Saito (1974), Pacific Pleistocene sediments: Planktonic foraminifera dissolution cycles and geochronology, *Geology*, *2*, 333–335.

Thunnell, R. C. (1976), Optimum indices of calcium calcite dissolution in deep sea sediments, *Geology*, *4*, 525–528.

R. François, Department of Earth and Ocean Sciences, University of British Columbia, Vancouver, British Columbia, Canada V6T 1Z4. (rfrancois@eos.ubc.ca)

F. Mekik, Department of Geology, Grand Valley State University, Allendale, MI 49401, USA. (mekikf@gvsu.edu)